ACS Medicinal Chemistry Letters

Letter

pubs.acs.org/acsmedchemlett

Potent and Selective Inhibitors of CK2 Kinase Identified through Structure-Guided Hybridization

James E. Dowling,* Claudio Chuaqui, Timothy W. Pontz, Paul D. Lyne, Nicholas A. Larsen, Michael H. Block, Huawei Chen, Nancy Su, Allan Wu, Daniel Russell, Hannah Pollard, John W. Lee, Bo Peng, Kumar Thakur, Qing Ye, Tao Zhang, Patrick Brassil, Vicki Racicot, Larry Bao, Christopher R. Denz, and Emma Cooke

AstraZeneca, Oncology Innovative Medicines Unit, 35 Gatehouse Drive, Waltham, Massachusetts 02145, United States

Supporting Information

ABSTRACT: In this paper we describe a series of 3-cyano-5-aryl-7-aminopyrazolo[1,5-*a*]-pyrimidine hits identified by kinase-focused subset screening as starting points for the structure-based design of conformationally constrained 6-acetamido-indole inhibitors of CK2. The synthesis, SAR, and effects of this novel series on Akt signaling and cell proliferation *in vitro* are described.

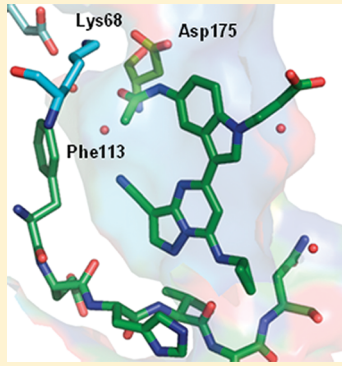

KEYWORDS: *CK2, casein kinase, structure-based design, pyrazolo[1,5-a]pyrimidine*

Casein Kinase 2 (CK2) is a highly conserved and ubiquitously expressed serine/threonine kinase, which exists as a tetrameric complex containing two catalytic (α or α') and two regulatory (β) subunits.[1] CK2 is regarded as a constitutively active kinase with broad function, although more recent evidence suggests that CK2 can be regulated by growth factors such as IL-6 and epidermal growth factor (EGF).[2,3] The importance of CK2 for cell viability has been demonstrated by genetic studies, showing that suppression of the α or β subunits leads to embryonic lethality in mice, while genetic silencing of the α' subunit results in viable offspring, but with males exhibiting defects in spermatogenesis leading to infertility.[4,5] CK2 regulates several key oncogenic signaling pathways, including PI3K (phosphatidylinositol 3-kinase), AKT (protein kinase B), NFκB (nuclear factor kappa-light-chain-enhancer of activated B cells), and Wnt (wingless type MMTV integration site family).[6−8] Targeted overexpression in transgenic animal models results in neoplastic growth[9] and administration of antisense oligodeoxy nucleotides against CK2α induced concentration-dependent tumor shrinkage in a human prostate cancer xenograft model.[10]

A variety of ATP-competitive, small molecule inhibitors of CK2 have been identified.[11] These include various polyhydroxylated aromatic compounds, such as emodin and quercetin, polyhalogenated compounds, such as DRB (5,6-dichlororibofuranosylbenzimidazole) and TBB (4,5,6,7-tetrabromo-1H-benzotriazole), as well as the indolo[1,2-*a*]quinazoline derivative IQA.[12] More recently, researchers from Cylene have disclosed CX-4945, a selective, orally available small molecule inhibitor of CK2 which exhibits single-agent activity in xenograft models and is currently in clinical trials for the treatment of cancer.[13]

There remains a need for additional novel agents with the necessary balance of potency, selectivity, druglike properties, tolerability, and efficacy that can successfully exploit the critical function of CK2 in cancer-linked pathways for the treatment of disease. Herein we disclose the discovery of a series of potent and selective inhibitors of CK2 derived from the pyrazolo[1,5-*a*]-pyrimidine scaffold.

As an alternative to conventional high throughput screening (HTS), we employed a kinase-focused subset screening approach. A library of ≈10K compounds was assembled from the AstraZeneca collection by applying general kinase binding-site and target-specific structural bioinformatic filters. Single point screening of the subset gave ≈2500 compounds with kinase inhibiton greater than 60% at 10 μM. These hits were consolidated further by application of physical property, *in vitro* ADME (absorption, distribution, metabolism, and excretion), and kinase selectivity filters to give ≈1400 compounds selected for full CK2 α' IC_{50} determination using an *in vitro* mobility shift microfluidics assay.[14] Among the hits characterized in this way, a series of 3-cyano-5-aryl-7-amino-pyrazolo[1,5-*a*]pyrimidines (Table 1, **1a**−**h**) exhibited submicromolar potency and high

Received: October 27, 2011
Accepted: January 24, 2012
Published: January 24, 2012

Table 1. CK2 Biochemical and Cellular Potency for Compounds 1a−h and 3a−h

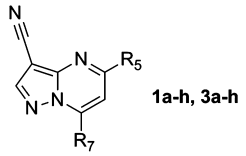

cpd	R_5	R_7	CK2 IC_{50} (μM)[a]	HCT-116 GI_{50} (μM)[a]
1a	2-thienyl	NH_2	0.10	>30
1b	Ph	NH_2	0.18	>30
1c	*p*-MeO-Ph	NH_2	0.058	ND
1d	*p*-F-Ph	NH_2	0.43	ND
1e	2-thienyl	cyclopropylamino	0.46	ND
1f	*p*-MeO-Ph	cyclopropylamino	0.078	14
1g	*p*-MeO-Ph	1-methyl-1H-pyrazol-3-ylamino	0.052	4.5
1h	4-methoxy-3-pyridyl	cyclopropylamino	0.25	16 (15)[b]
3a	6-acetamidoindol-1-yl	cyclopropylamino	0.010	0.53 (1.0)[b]
3b	6-acetamidoindazol-1-yl	cyclopropylamino	0.026	3.7 (5.0)[b]
3c	6-acetamido-pyrrolo[3,2-*b*]pyridin-1-yl	cyclopropylamino	<0.003	3.0 (2.1)[b]
3d	6-acetamidoindolin-1-yl	cyclopropylamino	0.004	0.53 (0.73)[b]
3e	6-acetamido-(3,4-dihydro-2H-benzo[*b*][1,4]oxazin-4-yl)-	cyclopropylamino	0.27	ND
3f	6-acetamido-(1,2,3,4-tetrahydroquinolin-7-yl)-	cyclopropylamino	0.24	ND
3g	6-acetamido-5-methyl-indol-1-yl	cyclopropylamino	0.079	>30
3h	6-acetamido-indol-1-yl	1-methyl-1H-pyrazol-3-ylamino	0.024	0.46 (0.56)[b]

[a]Mean value of three experiments. Deviations were within < ±25%. [b]SW480 Alamar Blue proliferation assay; ND = not determined.

ligand efficiency[15] (**1a**; LE = 0.4). Preliminary SAR studies for **1a−h** suggested that electron-rich aromatic and heteroaromatic systems at C5 and substitution of the C7 amine with small carbo- and heterocyclic substituents enhanced potency. Neither the des-cyano analogue of **1a** nor the 2-methyl derivative of **1f** (not shown) exhibited activity toward CK2 (>30 μM). However, despite the encouraging biochemical activity exhibited by this series, potency in Alamar Blue cell proliferation assays[14] was modest (**1g**, HCT-116 GI_{50} = 4.5 μM).

During the course of this effort, a disclosure[16] by other researchers described a series of CK2 inhibitors (**2**) with pharmacophoric elements designed to establish interactions with Lys^{68}, Asp^{175}, and a previously observed structural water molecule.[12] We sought to couple these insights with further modifications identified in our own work. *In silico* modeling of **1a** with compound **2** (Figure 1) suggested the introduction of acetamide-containing 5,6-fused ring systems at the C5 position of the pyrazolo[1,5-*a*]pyrimidine core to give conformationally constrained hybrid structures such as **3a** (Figure 2).

To test this design hypothesis, we prepared a series of 3-cyano-7-cyclopropylamino-pyrazolo[1,5-*a*]pyrimidines substituted at the 5-position with various 5,6- and 6,6-fused ring heterocycles (Table 1). Gratifyingly, indole **3a** (CK2 IC_{50} = 10 nM) demonstrated that a planar, bicyclic structure is accommodated by the receptor and that the aniline NH of **2** is less important for its activity. Introduction of nitrogen into the five-membered ring, as with indazole **3b**, led to a modest reduction in potency whereas 4-azaindole derivative **3c** exhibited enhanced enzymatic potency relative to **3a**. Partial saturation of the five-membered ring, as with indoline **3d**, preserved activity; however, partially saturated 6,6-fused analogues such as benzoxazine **3e** and tetrahydroquinoline **3f** are 10-fold less active. Substitution adjacent to the acetamide, as in 5-methyl derivative **3g**, is disfavored, presumably due to destabilization of the interaction with Lys^{68} and Asp^{175} via increased out-of-plane rotation. Deletion of the 3-cyano group in **3a** (not shown) led to a significant reduction in enzymatic activity (CK2 IC_{50} = 2.6 μM).

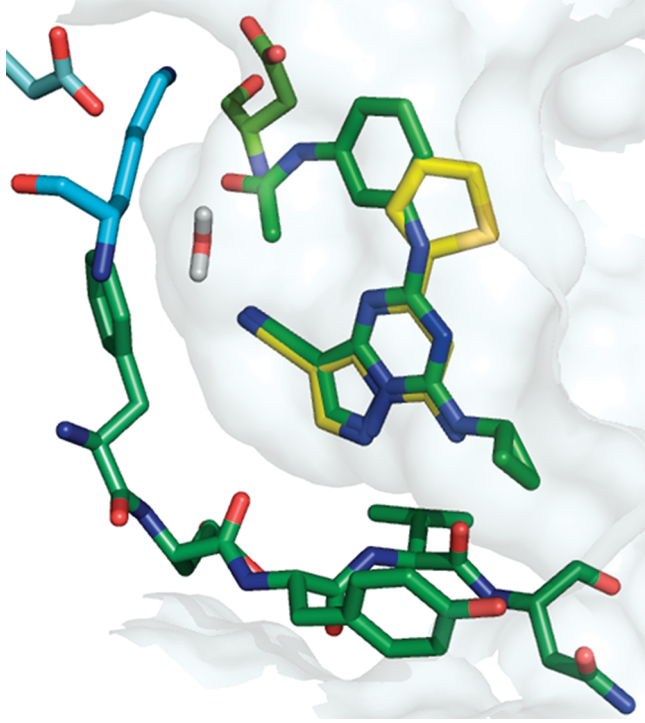

Figure 1. Overlay of screening hit **1a** with compound **2** illustrating their computationally derived binding poses in CK2.

Cellular potency for this series was determined using mechanistic and phenotypic end points. Depletion of cellular levels of $pAKT^{S129}$, a direct substrate of CK2 believed to hyperactivate the AKT pathway,[7] was measured in Western blot and ELISA (enzyme-linked immunosorbent assay) formats (Figure 3).[17] Consistent with effects on prosurvival signaling, **3a** induces

dx.doi.org/10.1021/ml200257n | *ACS Med. Chem. Lett.* 2012, 3, 278−283

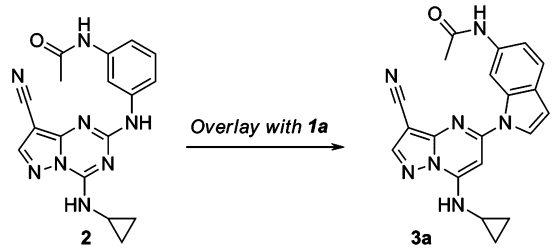

Figure 2. Design of fused-ring analogue **3a**.

apoptosis, as measured by caspase activation in HCT-116 cells (not shown). Indole **3a** and indoline **3d** possess comparable antiproliferative activity. However, for reasons not clear to us, indazole **3b** and 4-azaindole derivative **3c** exhibit a 30−100-fold drop in phenotypic potency relative to the effects observed in the pAKT^{S129} ELISA assay. Comparable potency was exhibited in a SW480 cell proliferation assay.

The physical properties for **3a**−**h** are poor, with low aqueous solubility, high protein binding in human plasma, and moderate lipophilicity (**3a**; solubility <10 μM at pH 7, fu <1%, log D = 3.3). As a consequence, the *in vivo* pharmacokinetic profile for **3a** following a single oral 10 mg/kg dose in the rat is characterized by poor oral bioavailability (F = 5%) and low clearance (Cl = 10 mL/(min/kg)). In addition, **3a** possesses moderate activity at the hERG (human *Ether-a-go-go* Related Gene) ion channel (hERG IC_{50} = 8.6 μM) and inhibits CYP1A2 (cytochrome p450 isozyme) with an IC_{50} = 0.1 μM. Conversely, indazole **3b** and indoline **3d** exhibit reduced hERG channel activity (hERG IC_{50} >33 μM) while 4-azaindole **3c** is devoid of CYP1A2 activity (CYP1A2 IC_{50} > 20 μM).

We next attempted to improve the physical properties in **3a** by replacing the N7 cyclopropyl substituent with hydrophilic groups. Analysis of the ATP-binding site suggested that several residues in the solvent channel are potentially disposed to form favorable interactions with polar groups and may also serve as selectivity determinants against other kinases. On the basis of the SAR for the indole and related heterocycles, we felt that we could optimize cellular potency and physical properties through modifications in other portions of the structure and potentially employ the indoline or 4-azaindazole rings to address *in vitro* ADME issues should they persist.

Replacement of the cyclopropyl group of **3a** with four- and five-membered heterocycles is well-tolerated; *N*-methylpyrazole **3h** exhibits cellular potency equivalent to that of **3a** (pAKT IC_{50} = 16 nM) while oxetane **4a** is 4-fold less active (Table 2). Hydrophilic substituents at the terminus of two- and three-atom spacers preserved enzymatic activity and enhanced physical properties but led to significant reduction in cellular potency. Despite possessing comparable enzymatic activity with **3h**, 1-hydroxybutyl derivative **4b** and dimethylamino-propyl derivative **4e** exhibit a 10- and 100-fold drop in potency in the mode of the action assay (pAKT^{S129} ELISA), respectively. The permeability of **3a** in MDCK-MDR1 (multidrug resistance protein 1) cells is moderate (A-B Papp = 22 × 10^{-6} cm/s) with low efflux characteristics (efflux ratio = 1.4). Conversely, both **4c** and **4f** exhibit low A-B permeability (A-B Papp ≤5 × 10^{-6} cm/s) and high efflux potential (efflux ratio = 17) in MDR1 overexpressing LLC/PK1 cells. In addition, compound **4f** exhibits virtually no exposure (AUC = 0.065 μM·h) following administration of a single 10 mg/kg oral dose in the rat. These results suggest that membrane permeation in this series is impaired when lipophilicity is reduced such that log D < 2.9, and the effect may be compounded by the presence of a basic amine.

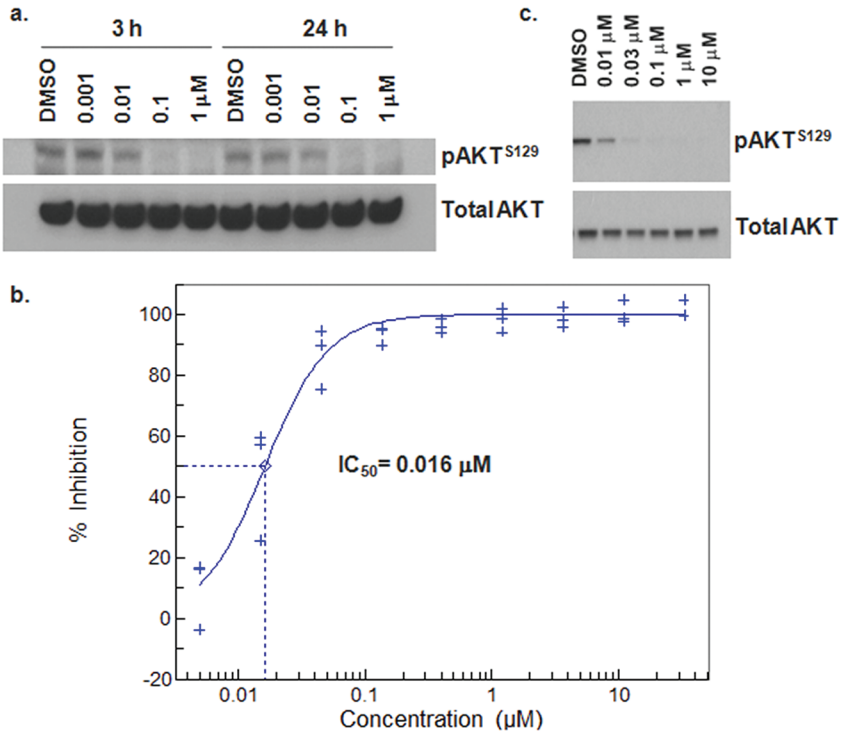

Figure 3. (a) Concentration-dependent depletion of pAKT^{S129} in HCT-116 cells at 3 h and 24 h by **3a**, as measured by Western blot analysis. (b) Inhibition of pAKT^{S129} in DLD-1 cells by **3h** as determined by ELISA. (c) Depletion of pAKT^{S129} in DLD-1 cells upon treatment with **3h** at 24 h as determined by Western blot.

dx.doi.org/10.1021/ml200257n | *ACS Med. Chem. Lett.* 2012, 3, 278−283

Table 2. CK2 Biochemical and Cellular Potency and Physical Property Data for Indoles 4a−4i

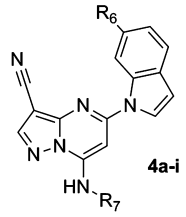

cpd	R_7	R_6	CK2 IC_{50} (μM)[a]	pAKT IC_{50} (μM)[a]	HCT-116 GI_{50} (μM)[a]	log *D*	sol (μM)	Hu PPB Fu (%)
4a	oxetan-3-yl	AcNH	0.004	0.057	2.2 (2.5)[b]	2.2	1	12.4
4b	4-hydroxybutyl	AcNH	0.030	0.19	2.8	2.6	8	4.1
4c	2-morpholinoethyl	AcNH	0.03	0.46	>30[b]	ND	2	11
4d	2-(pyrrolidin-1-yl)ethyl	AcNH	0.04	0.78	ND	2.2	15	5.6
4e	3-(dimethylamino)propyl	AcNH	0.030	1.2	25[b]	1.6	750	10
4f	3-(pyrrolidin-1-yl)propyl	AcNH	0.018	0.86	13[b]	1.8	>1000	6.7
4g	cyclopropyl	AcNMe	0.011	0.034	ND	2.9	<1	2.5
4h	cyclopropyl	$HOCH_2$	0.12	0.83	10.1	3.1	<1	1.9
4i	cyclopropyl	$MeSO_2CH_2$	0.007	0.083	16.4	2.5	<1	1.8

[a]Mean value of at least three experiments. [b]SW480 Alamar Blue cell proliferation assay; ND = not determined.

Table 3. CK2 Biochemical and Cellular Potency for 5a−f

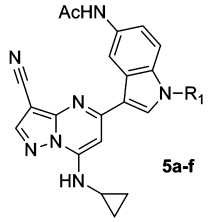

cpd	R_1	CK2 IC_{50} (nM)[a]	pAKT IC_{50} (μM)[a]	HCT-116 GI_{50} (μM)[a]
5a	Me	6	0.027	0.7 (1.1)[b]
5b	H	5	0.077	0.7 (0.7)[b]
5c	2-hydroxyethyl	<3	0.50	2.7 (4.5)[b]
5d	3-hydroxypropyl	<3	0.21	2.3 (3.2)[b]
5e	$CH_2CH_2CO_2Me$	15	ND	6.6[b]
5f	$CH_2CH_2CO_2H$	<3	3.1	ND

[a]Mean value of at least three experiments. [b]SW480 Alamar Blue cell proliferation assay; ND = not determined.

We next focused on modifying the acetamide to address the observed drop-off in cellular potency and the low bioavailability of nonbasic compounds. Substitution of the acetamide NH of **3a**, to give *N*-methylacetamide **4g**, preserved enzymatic and cellular activity but led to reduced stability when incubated with rat liver microsomes (Cl_{int} = 100 mL/(min/kg)). Installation of a hydroxymethyl group (**4h**) led to a significant reduction in enzymatic and cellular potency. Sulfone **4i** exhibited high potency in the biochemical assay and moderate activity in the pAKT assay but lacked any significant antiproliferative effect. These results also confirm the pivotal role of the acetamide carbonyl of **3a** and suggest that the NH is less critical and that other variations on the donor−acceptor group may be tolerated.

As an alternative to the solvent channel approach, we explored the use of a "reversed" indole scaffold to incorporate polar functionality (Table 3). The N1-methyl analogue (**5a**) and the unsubstituted **5b** are potent CK2 inhibitors and exhibit submicromolar activity in the proliferation assay. More elaborate substitution at this position gave compounds (**5c−f**) with high enzyme activity but weaker effects in the mode of action ($pAKT^{S129}$) and phenotypic assays.

An X-ray cocrystal structure determination of **5f** with recombinant human CK2 at 2.2 Å resolution showed the inhibitor bound as anticipated with N2 of the pyrazolo[1,5-*a*]-pyrimidine core and the C7 NH interacting at the hinge region of the ATP binding pocket.[17] As indicated in Figure 4, the energetic penalty associated with adopting the *cis*- conformation of the acetamide is compensated by a network of hydrogen bonding interactions with Lys^{68} and Asp^{175} via the carbonyl and NH, respectively. Moreover, a buried water molecule in the vicinity of the gatekeeper residue (Phe^{113}) is coordinated by the acetamide carbonyl (2.7 Å) and the cyano group (3.0 Å). The propanoic acid adopts an extended conformation in which the β-CH_2 group makes a hydrophobic contact between Gly^{46} and the side-chain of Val^{53} and positions the carboxylate group at the solvent-accessible surface.

CK2 shares a high degree of binding site homology with a range of kinases, including GSK-3β (glycogen synthase kinase 3 beta) and CDK2 (cyclin-dependent kinase 2), targets for which pyrazolo[1,5-*a*]pyrimidine derivatives are reported to have affinity.[18] Compound **3a** was shown to be highly selective when tested against a panel of 324 kinases (Ambit Biosciences, San Diego, CA),[19] at a concentration of 1 μM. From the 16 kinases with inhibition >50%, we selected four for subsequent IC_{50} determinations (Table 4). Introduction of nitrogen reduces affinity toward GSK-3β, as in indazole **3b** (IC_{50} = 0.7 μM) and

dx.doi.org/10.1021/ml200257n | ACS Med. Chem. Lett. 2012, 3, 278−283

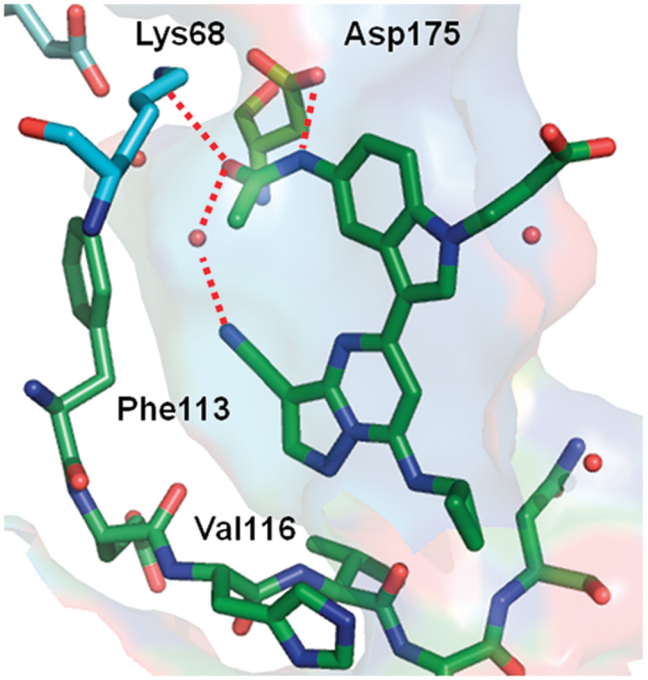

Figure 4. X-ray cocrystal structure determination of **5f** with huCK2 at 2.2 Å. Bound water molecules are shown as spheres.

Table 4. Kinase Selectivity Data for 3a and Related Compounds

cpd	GSK-3β IC_{50} (μM)	HipK2 IC_{50} (μM)	Dyrk1 IC_{50} (μM)	CDK2 IC_{50} (μM)
3a	0.13	0.03	0.8	26
3b	0.7	0.05	0.02	>30
3c	1.0	0.02	1.7	>30
4e	2.6	0.06	2.6	>30
4g	1.4	<0.003	0.4	>30
5b	0.25	<0.003	0.06	14
5f	6	0.57	5.4	>30

4-azaindole **3c** (IC_{50} = 1.0 μM). The presence of a basic group in the solvent channel region, as in **4e**, reduces GSK-3β (IC_{50} = 2.6 μM) and Dyrk1 (dual-specificity tyrosine phosphorylation-regulated kinase 1) activity (IC_{50} = 2.6 μM). Members of the series exhibit a high degree of HipK2 (homeodomain-interacting protein kinase 2) potency, although substitution of the "reversed" indole NH reduces this affinity (**5f**, HipK2 IC_{50} = 0.57 μM). These data suggest that further enhancement of CK2 selectivity in this scaffold may be achieved through appropriate combination of the diversity elements identified thus far.

Synthesis of 5-acetamidoindole and related analogues (**3a–h**, **4a–i**) was accomplished using a convergent approach (Scheme 1) that commenced with installation of the requisite amine by displacement of the 7-chloro group in 5,7-dichloro-3-cyanopyrazolo[1,5-*a*]pyrimidine (**6**). Replacement of the 5-chloro substituent in **7** was accomplished by $Pd_2(dba)_3$ (tris(dibenzylideneacetone)dipalladium(0))-mediated coupling via the NH of the appropriate fused ring system.[20] In cases where the acetamide was not yet present in the coupling partner, the appropriate nitro precursor precursor (**8**, **11**, **13**) was utilized followed by subsequent reduction (to give **9**, **12**, and **14**, respectively) and acetylation. Similarly, methylsulfonylmethyl derivative **4h** was prepared from **4g** followed by mesylation and displacement with $MeSO_2Na$. Synthesis of "reversed" indoles (**5a–f**) was carried out beginning with the *p*-toluenesulfonyl derivative of 5-nitroindole (**15**) followed by conversion to mercury(II)acetate derivative **16** and subsequent treatment with borane to afford boronic acid **17**.

Suzuki coupling of the latter with **7** afforded **18**, which, following functional group manipulation, gave a mixture of **5a** and **5b**. Alkylation of the indole NH could be accomplished to deliver **5c** and **5d**. Conjugate addition of **5b** with methyl methacrylate furnished **5e**, which afforded **5f** following ester hydrolysis (Scheme 2).

In conclusion, we have identified a series of potent and selective inhibitors of CK2 kinase using structure-based hybridization of an early screening hit with a literature scaffold. Enhancement of physical properties in the 6-acetamidoindole series (**3a**) was achieved by modification of the N7 substituent

Scheme 1[a]

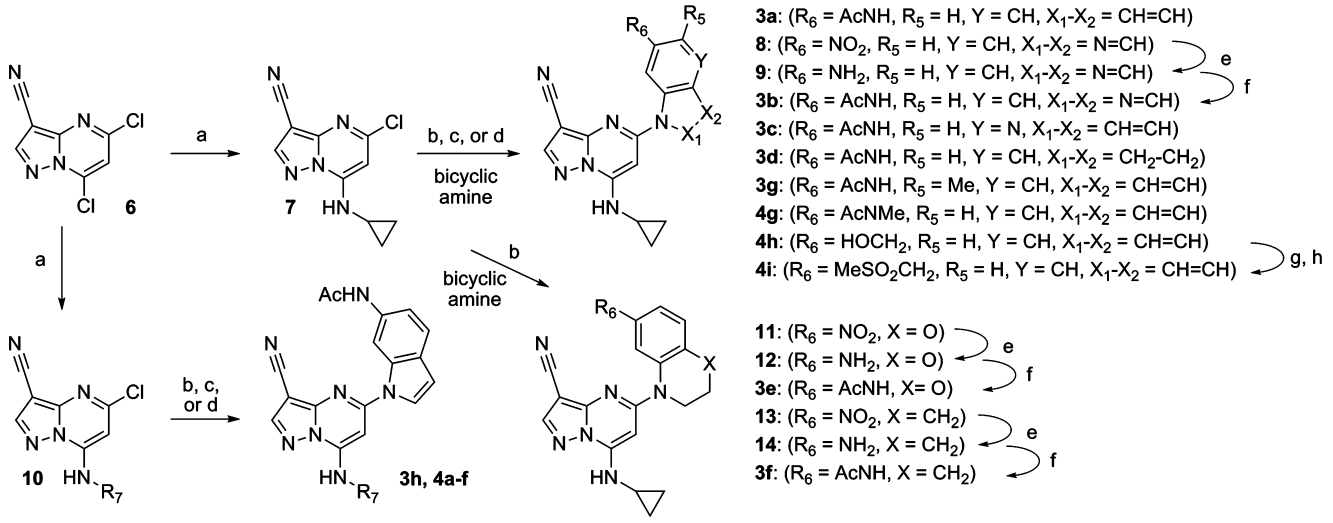

[a]Reagents and conditions: (a) R_7-NH_2, EtOH, 25 °C; (b) $Pd(OAc)_2$, Xantphos, Cs_2CO_3, DMA (*N*,*N*-dimethyl acetamide)/H_2O (4:1), 150 °C, microwave, 0.5 h; (c) $Pd_2(dba)_3$, Xantphos, Cs_2CO_3, DMA/H_2O (4:1), 150 °C, microwave, 0.5 h; (d) $Pd_2(dba)_3$, Xantphos, Cs_2CO_3, 1,4-dioxane, 150 °C, microwave, 0.5 h; (e) H_2, Pd/C; (f) Ac_2O, pyridine, 25 °C; (g) DIEA (*N*,*N*-diisopropylethylamine), MsCl, THF; (h) KI, $MeSO_2Na$, DMF, 25 °C.

dx.doi.org/10.1021/ml200257n | ACS Med. Chem. Lett. 2012, 3, 278–283

Scheme 2[a]

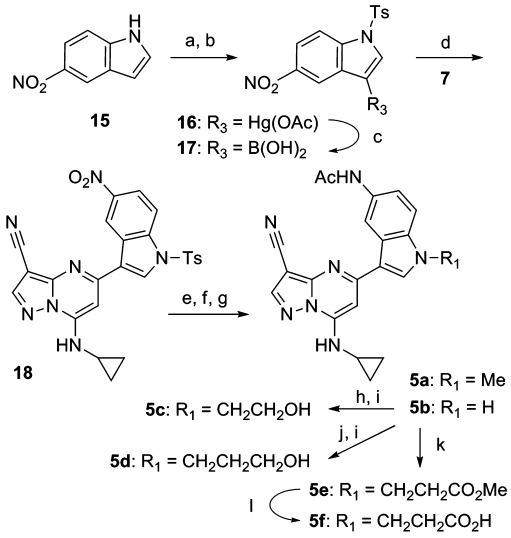

[a]Reagents and conditions: (a) TsCl, Bu_4NHSO_4, PhMe, 50% aq NaOH; (b) $Hg(OAc)_2$, HOAc, $HClO_4$; (c) BH_3, H_2O; (d) $Pd(PPh_3)_4$, Na_2CO_3, 1,4-dioxane, 100 °C, 3 h; (e) H_2, Pd/C, DMF/MeOH; (f) Ac_2O, pyridine, 25 °C; (g) Cs_2CO_3, MeOH, THF; (h) [(3-bromoethyl)oxy](1,1-dimethylethyl) dimethylsilane, K_2CO_3, DMF, 100 °C, microwave; (i) HCl (4.0 M in 1,4-dioxane), 25 °C; (j) [(3-bromopropyl)oxy](1,1-dimethylethyl)dimethylsilane, K_2CO_3, DMF, 100 °C, microwave; (k) methyl acrylate, DBU (1,8-diazabicyclo[5.4.0]undec-7-ene), MeCN, 25 °C; (l) LiOH, THF, MeOH, H_2O, 25 °C.

but had a deleterious effect on cellular potency. Kinase selectivity profiling has revealed **3a** to be highly selective and has identified structural features that further reduce off-target effects. Exploitation of the crystallographically determined binding mode of **5f** for enhancement of primary target potency and kinase selectivity will be described in a subsequent communication.

■ ASSOCIATED CONTENT

Ⓢ Supporting Information

Representative experimental procedures for synthesis of analogues, biochemical and cellular assays, and X-ray structure determination. This material is available free of charge via the Internet at http://pubs.acs.org.

■ AUTHOR INFORMATION

Corresponding Author

*Telephone: 781-839-3900. E-mail: james.dowling@astrazeneca.com.

Notes

The authors declare no competing financial interest.

■ REFERENCES

(1) Pinna, L. A. Protein kinase CK2: a challenge to canons. *J. Cell Sci.* **2002**, *115*, 3873−3878.

(2) Allende, J. E.; Allende, C. C. Protein kinases 4. Protein kinase CK2: an enzyme with multiple substrates and a puzzling regulation. *FASEB J.* **1995**, *9*, 313−323.

(3) Ji, H.; Wang, J.; Nika, H.; Hawke, D.; Keezer, S.; Ge, Q.; Fang, B.; Fang, X.; Litchfield, D. W.; Aldape, K. EGF-induced ERK activation promotes CK2-mediated disassociation of alpha-catenin from beta-catenin and transactivation of beta-catenin. *Mol. Cell* **2009**, *36*, 547−559.

(4) Lou, D. Y.; Dominguez, I.; Toselli, P.; Landesman-Bollag, E.; O'Brien, C.; Seldin, D. C. The alpha catalytic subunit of protein kinase CK2 is required for mouse embryonic development. *Mol. Cell. Biol.* **2008**, *28*, 131−139.

(5) Buchou, T.; Vernet, M.; Blond, O.; Jensen, H. H.; Pointu, H.; et al. Disruption of the regulatory beta subunit of protein kinase CK2 in mice leads to a cell-autonomous defect and early embryonic lethality. *Mol. Cell. Biol.* **2003**, *23*, 908−915.

(6) Ruzzene, M.; Pinna, L. A. Addiction to protein kinase CK2: A common denominator of diverse cancer cells? *Biochim. Biophys. Acta* **2010**, *1804*, 499−504.

(7) Di Maira, G.; Brustolon, F.; Pinna, L. A.; Ruzzene, M. Dephosphorylation and inactivation of Akt/PKB is counteracted by protein kinase CK2 in HEK 293T cells. *Cell. Mol. Life Sci.* **2009**, *66*, 3363−3373.

(8) Dominguez, I.; Sonenshein, G. E.; Seldin, D. C. CK2 and its role in Wnt and NF-kappa B signaling: Linking development and cancer. *Cell. Mol. Life Sci.* **2009**, *66*, 1850−1857.

(9) Landesman-Bollag, E.; Romieu-Mourez, R.; Song, D. H.; Sonenshein, G. E.; Cardiff, R. D.; Seldin, D. C. Protein kinase CK2 in mammary gland tumorigenesis. *Oncogene* **2001**, *20*, 3247−3257.

(10) Slaton, J. W.; Unger, G. M.; Sloper, D. T.; Davis, A. T.; Ahmed, K. Induction of apoptosis by antisense CK2 in human prostate cancer xenograft model. *Mol. Cancer Res.* **2004**, *2*, 712−721.

(11) Duncan, J. S.; Litchfield, D. W. Too much of a good thing: the role of protein kinase CK2 in tumorigenesis and prospects for therapeutic inhibition of CK2. *Biochim. Biophys. Acta* **2007**, *1784*, 33−47.

(12) Battistutta, R. Structural basis of protein kinase CK2 inhibition. *Cell. Mol. Life Sci.* **2009**, *66*, 1868−1889.

(13) Pierre, F.; Chua, P. C.; O'Brien, S. E.; Siddiqui-Jain, A.; Bourbon, P.; Haddach, M.; Michaux, J.; Nagasawa, J.; Schwaebe, M. K.; Stefan, E.; Vialettes, A.; Whitten, J. P.; Chen, T. K.; Darjania, L.; Stansfield, R.; Anderes, K.; Bliesath, J.; Drygin, D.; Ho, C.; Omori, M.; Proffitt, C.; Streiner, N.; Trent, K.; Rice, W. G.; Ryckman, D. M. Discovery and SAR of 5-(3-chlorophenylamino)benzo[c][2,6]-naphthyridine-8-carboxylic acid (CX-4945), the first clinical stage inhibitor of protein kinase CK2 for the treatment of cancer. *J. Med. Chem.* **2011**, *54*, 635−54.

(14) See Supporting Information.

(15) Bembenek, S. D.; Tounge, B. A.; Reynolds, C. H. Ligand efficiency and fragment-based drug discovery. *Drug Discovery Today* **2009**, *14*, 278−283. LE (ligand efficiency) = −log(CK2 IC_{50})/number of heavy atoms.

(16) Nie, Z.; Perretta, C.; Erickson, P.; Margosiak, S.; Almassy, R.; Lu, J.; Averill, A.; Yager, K. M.; Chu, S. Structure-based design, synthesis, and study of pyrazolo[1,5-a][1,3,5]triazine derivatives as potent inhibitors of protein kinase CK2. *Bioorg. Med. Chem. Lett.* **2007**, *17*, 4191−4195.

(17) The PDB deposition code for the cocrystal structure is 3U4U.

(18) Williamson, D. S.; Parratt, M. J.; Bower, J. F.; Moore, J. D.; Richardson, C. M.; Dokurno, P.; Cansfield, A. D.; Francis, G. L.; Hebdon, R. J.; Howes, R.; Jackson, P. S.; Lockie, A. M.; Murray, J. B.; Nunns, C. L.; Powles, J.; Robertson, A.; Surgenor, A. E.; Torrance, C. J. Structure-guided design of pyrazolo[1,5-a]pyrimidines as inhibitors of human cyclin-dependent kinase 2. *Bioorg. Med. Chem. Lett.* **2005**, *15*, 863−867.

(19) Karaman, M. W.; Herrgard, S.; Treiber, D. K.; Gallant, P.; Atteridge, C. E.; Campbell, B. T.; Chan, K. W.; Ciceri, P.; Davis, M. I.; Edeen, P. T.; Faraoni, R.; Floyd, M.; Hunt, J. P.; Lockhart, D. J.; Milanov, Z. V.; Morrison, M. J.; Pallares, G.; Patel, H. K.; Pritchard, S.; Wodicka, L. M.; Zarrinkar, P. P. A quantitative analysis of kinase inhibitor selectivity. *Nat. Biotechnol.* **2008**, *26*, 127−132.

(20) Kranenburg, M.; van der Burgt, Y. E. M.; Kamer, P. C. J.; van Leeuwen, P. W. N. M.; Goubitz, K.; Fraanje, J. New diphosphine ligands based on heterocyclic aromatics inducing very high regioselectivity in rhodium-catalyzed hydroformylation: effect of the bite angle. *Organometallics* **1995**, *14*, 3081−3089.